Supporting Information to

Collectively Induced Quantum-Confined Stark Effect in Monolayers of Molecules Consisting of Polar Repeating Units

Ferdinand Rissner[†,||], *David A. Egger*[†,||], *Amir Natan*[‡,a], *Thomas Körzdörfer*[§], *Stephan Kümmel*[§], *Leeor Kronik*[‡], *and Egbert Zojer*[*,†]

[†] Institute of Solid State Physics, Graz University of Technology, 8010 Graz, Austria

[‡] Department of Materials and Interfaces, Weizmann Institute of Science, 76100 Rehovoth, Israel

[§] Theoretical Physics IV, University of Bayreuth,95440 Bayreuth, Germany

[a] current address: Department of Physical Electronics, Tel-Aviv University, 69978 Tel-Aviv, Israel

[||] These authors contributed equally to this work.
[*] To whom correspondence should be addressed: egbert.zojer@tugraz.at

S1: Detailed discussion of the role of self-interaction in terpyrimidinethiol.

The self-interaction error (SIE) is intuitively related to the localization of an orbital as one might expect that a strongly localized orbital is subject to more spurious self-repulsion than a more delocalized one.[1] This trend has indeed been observed,[2,3] although the complete picture obtained from a detailed analysis of the various contributions to the error is more subtle (see ref. [4] and the following discussion). When energetically neighboring orbitals carry markedly different amounts of self-interaction energy, this can severely distort the electronic structure, i.e., change the ordering of these states.

Because we are not aware of any experimental data for thiolated oligopyrimidines to compare our calculations with, it is indispensable to carefully evaluate the theoretical modeling methods. To this end, we follow the strategy presented in ref. [2,3], where a simple-to-evaluate predictor for the presence of a strongly orbital-dependent SIE has been proposed. To date, it is applicable only to finite systems. The predictor calculates the SIE for each Kohn-Sham orbital, i.e., the amount of Coulomb self-repulsion that is not cancelled by exchange-correlation (xc) self-attraction. It is, per definition, given by:

$$e_i = < \varphi_i | v_H[|\varphi_i|^2] | \varphi_i > + < \varphi_i | v_{xc}[|\varphi_i|^2, 0] | \varphi_i > \quad , \quad (1)$$

where $v_H[|\varphi_i|^2]$ and $v_{xc}[|\varphi_i|^2, 0]$ denote the Hartree and the used exchange-correlation potential for each orbital charge density $|\varphi_i|^2$; as in ref. [2,3], we use the spin-polarized LDA (local density approximation) for v_{xc}.

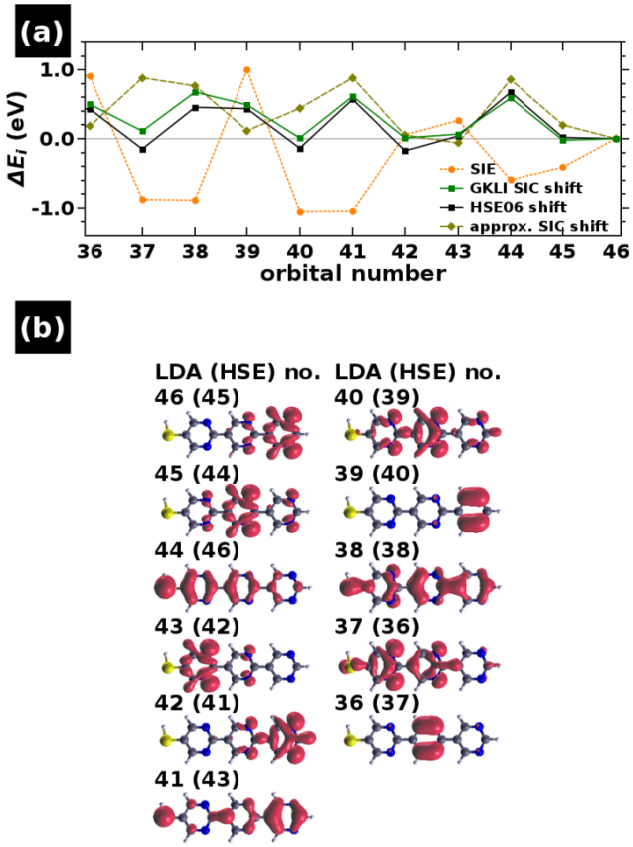

Fig. S1. Self-interaction error of the isolated $3N^{up}$ molecule. In (a), the self-interaction error of the LDA orbital energies according to eqn. (1) is shown (orange) together with the GKLI SIC (green), the HSE corrections (black) and the approximate SIC (eqn. (2), olive). All quantities are given relative to the value for the HOMO (orbital 46). (b) Orbital charge densities $|\varphi_i|^2$ for the 11 highest occupied LDA orbitals; HSE orbital indices are given in parenthesis.

The differences in the orbital SIE, e_i, relative to the value calculated for the HOMO level, $\Delta e_i \coloneqq (e_i - e_{46})$, are shown in orange color in Fig. S1 (reproduced from Fig. 2a). Real-space representations of the orbital charge densities $|\varphi_i|^2$ for the HOMO-10 to HOMO (i=36...46) are shown in Fig. S1b. From visual inspection, one can distinguish between orbitals mainly localized on one of the pyrimidine rings (no. 46, 45, 43, 42, 39, 36) and orbitals more delocalized over the molecular backbone (44, 41, 40, 38, 37), where both groups contain σ-

and π-states. The e_i essentially quantify this visual impression of localization: the largest Δe_i are found for orbitals 39 and 36; orbitals 46, 43 and 42 have a very similar Δe_i and decreasing values of Δe_i are found for the other orbitals with increasing delocalization. This is independent of the character of the orbitals (i.e., σ or π).

Typical routes to correct for self-interaction are to perform self-interaction correction (SIC)[2,3,5,6] or GW calculations.[7,8,9,10] Often, also hybrid functionals give satisfactory results,[7,5,11,12,8,13,14,15] although this is not purely due to self-interaction correction.[6] Hybrid functionals which include only a fraction of exact exchange only partially correct self-interaction. The reason for the often found good comparability with experiment and SIC or GW calculations for the low binding energy states is rather involved: In addition to the partial correction of self-interaction, the non-local potential operator part of hybrid functionals also partially circumvents another well-known deficiency of semi-local density functionals, namely the lack of derivative discontinuities in the exchange-correlation potential.[6] Moreover, it also partly mimics the non-local character of the self-energy operator in GW calculations.[16] The combination of these aspects then often results in the above-mentioned good comparability.

The relative orbital energy shifts $\Delta\varepsilon_i^{GKLI} \coloneqq (\varepsilon_i^{GKLI} - \varepsilon_i^{LDA}) - (\varepsilon_{HOMO}^{GKLI} - \varepsilon_{HOMO}^{LDA})$ obtained from a GKLI calculation and $\Delta\varepsilon_i^{HSE} \coloneqq (\varepsilon_i^{HSE} - \varepsilon_i^{LDA}) - (\varepsilon_{HOMO}^{HSE} - \varepsilon_{HOMO}^{LDA})$ obtained from an HSE calculation (see also main text) are depicted in Fig. S1a in green and black color, respectively. Different to Δe_i, the values of $\Delta\varepsilon_i^{GKLI}$ and $\Delta\varepsilon_i^{HSE}$ are primarily sensitive to the character of an orbital, i.e., there is a common correction for all σ- (no. 46, 45, 43, 42, 40, 37) and all π-states (no. 44, 41, 39, 38, 36), respectively, irrespective of the intuitive impression of localization quantified by Δe_i.

Perdew and Zunger[1] have proposed a simple-to-evaluate scheme for approximate SIC which proved surprisingly successful for organic semiconductor molecules in an adapted form.[2,3,4] It is interesting to evaluate the accuracy of this scheme for the present systems. Without actually going through the demanding procedure of self-consistent self-interaction correction, it can be evaluated solely on the basis of LDA quantities:

$$\varepsilon_i^{corr} = -0.94 \int (|\varphi_i|^2)^{4/3}\, d^3r - < \varphi_i | v_c^{LDA}[|\varphi_i|^2, 0] | \varphi_i >, \qquad (2)$$

where the estimated SIC-corrected eigenvalues are given as $\varepsilon_i^{LDA} + \varepsilon_i^{corr}$ in Rydberg units.[2,3] The values $\Delta\varepsilon_i^{corr} := (\varepsilon_i^{corr} - \varepsilon_{46}^{corr})$ are shown in Fig. S1a in brown color. It can be seen that the most important feature of GKLI/HSE, namely the shift of the HOMO-2 to above the LDA-HOMO, is reproduced in this approximation. This good agreement is, however, lost at higher binding energies.

S2. Further assessing the validity of the used DFT approach regarding a correct description of molecular polarizabilities, dipole moments and energy gaps.

Molecular polarizabilities, dipole moments and energy gaps are all quantities that are closely related to the effects described in the main manuscript. In literature, several instances have been discussed in which various flavors of density functional theory (DFT) fail in reliably describing these quantities (cf., main manuscript). To ensure that the trends in the main

manuscript are not adversely affected by such DFT shortcomings, we have performed a short comparative study calculating molecular polarizabilities and dipole moments using five different types of DFT functionals, Hartree Fock theory, and second order Møller-Plesset perturbation theory (MP2). As DFT functionals we chose the "classical" combination of Slater exchange[17] with the Vosko, Wilk, and Nusair 1980 correlation functional(III)[18] representing the local density approximation (LDA), the PBE[19,20] and PW91[21] functionals as typical generalized gradient approximation functionals, and B3LYP[22] and HSE06[23,24,25] from for the class of hybrid functionals. All test calculations have been performed using the Gaussian 03[26] (and for HSE06 Gaussian 09[27]) program suite choosing either the 6-31G(d,p) or the 6-311++G(d,p) basis set (in the latter case also using the "SCF=tight" keyword).

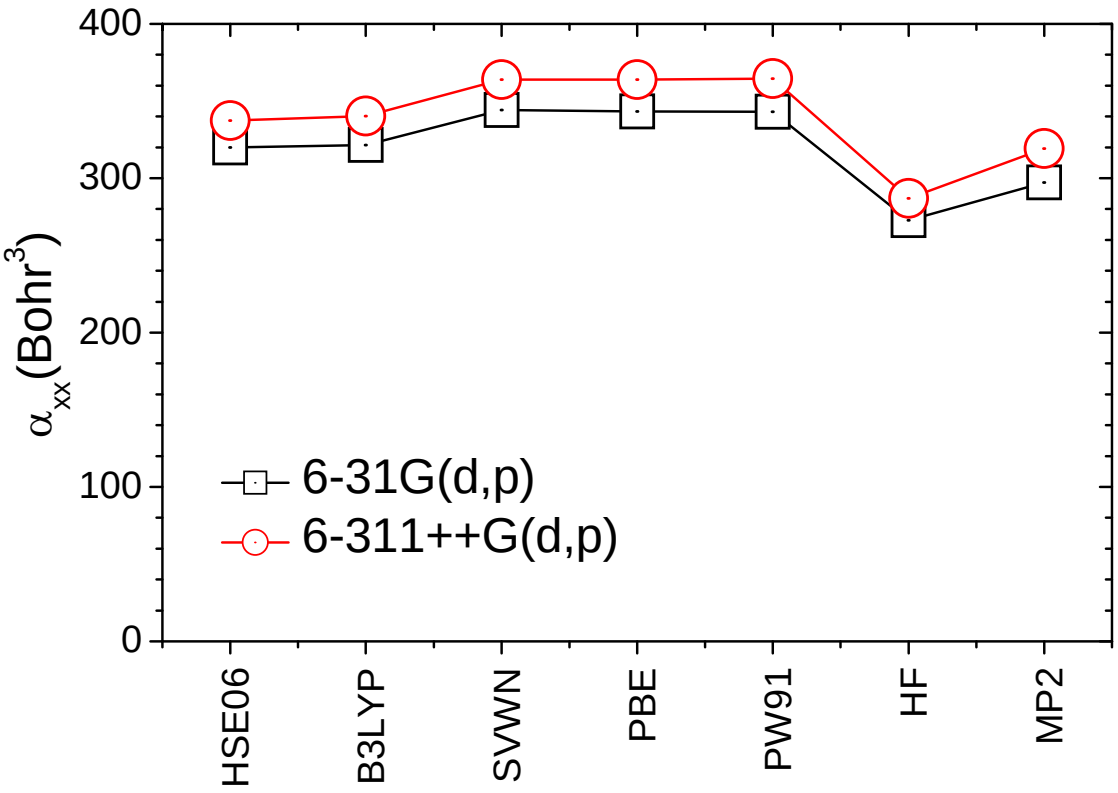

Fig. S2. Long axis molecular polarizabilities of terpyrimidine using different quantum-chemical approaches and basis sets (details see text) building on the B3LYP/6-31G(d,p) optimized geometry.

Table S1: *Long axis molecular polarizabilities ,α_{xx}, and molecular dipole moments, μ, of terpyrimidine using different quantum-chemical approaches and basis sets (details see text) building on the B3LYP/6-31G(d,p) optimized geometry.*

	α_{xx}(Bohr^3) 6-31G(d,p)	α_{xx}(Bohr^3) 6-311++G(d,p)	μ(Debye) 6-31G(d,p)	μ(Debye) 6-311++G(d,p)
HSE06	320.0	337.4	6.82	7.08
B3LYP	321.5	340.3	6.77	7.14
SVWN	344.2	363.9	6.87	7.28
PBE	343.3	363.9	6.58	6.98
PW91	343.1	364.5	6.60	7.02
HF	272.8	287.0	6.75	6.80
MP2	297.3	319.2	7.75	7.95

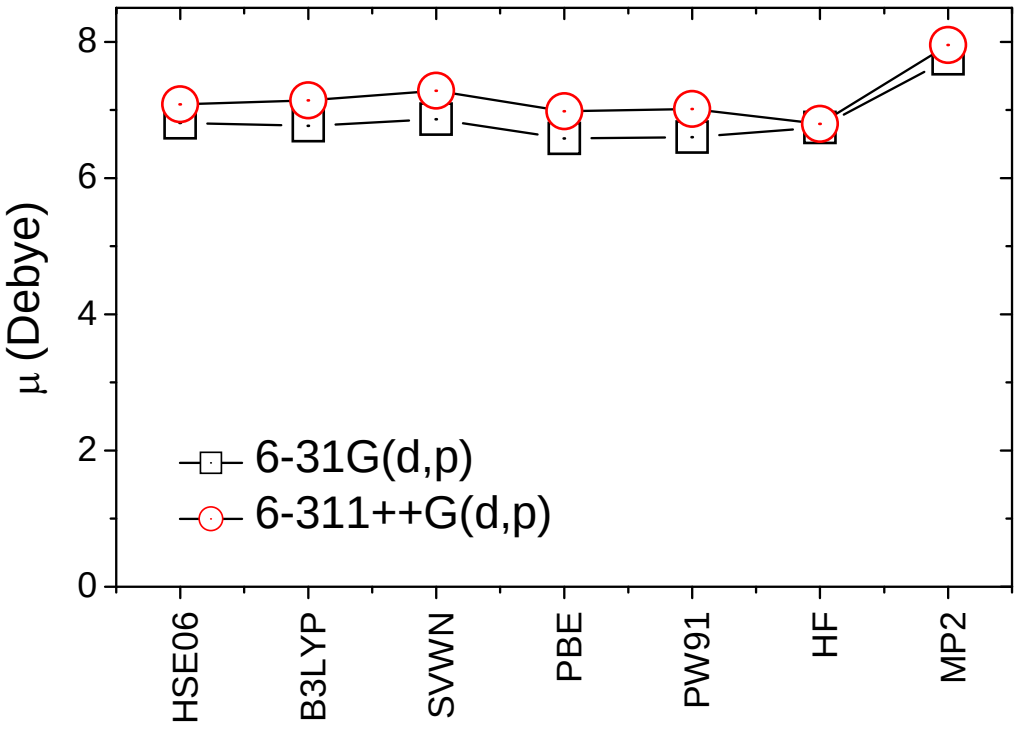

Fig. S3. Molecular dipoles of terpyrimidine using different quantum-chemical approaches and basis sets (details see text) building on the B3LYP/6-31G(d,p) optimized geometry.

As shown in Fig. S2 and Table S1, for terpyrimidine the DFT-calculated long-axis polarizabilities (obtained from a finite-field approach using the default settings in Gaussian) are only somewhat larger than those obtained from Hartree-Fock (HF) and MP2.

Amongst the DFT results, very similar values are obtained for the used GGA (PW91, PBE) functionals and for LDA (SVWN), while the hybrids (HSE06 and B3LYP) gives results that are closer to the HF and MP2 values, as expected due to the inclusion of exact exchange. Overall, the deviations are non-negligible but in no way of a magnitude that they would affect the conclusions drawn in the manuscript. For example, the HSE06 calculated α_{xx} is by only 6% larger than the MP2-calculated one, when using the 6-311++G(d,p) basis set. For the molecular dipoles, the variations are also small, as can be seen in Fig. S3. For example, the deviations between HSE and HF are between 0.3% and 5%. Only the MP2 values are larger (by ca. 11%).

Regarding the HOMO-LUMO gap, the situation is more involved. It is well known that the self-interaction error and the lack of derivative discontinuity of conventional functionals result in a severe underestimation of the gap when using density functional theory. This effect is mediated by the use of hybrid functionals as shown in Table S2. In fact, in terpyrimidine the HSE06 HOMO-LUMO gap is by ca. 0.5 eV larger than the optical gap calculated by time-dependent density functional theory, while the GGA and LDA functionals give rise to the expected severe underestimation.

Table S2: HSE/B3LYP calculated vertical ionization energies, electron affinities[i]*, IP-EA as well as optical gaps and HOMO and LUMO energies obtained using the specified functionals and basis sets. All energies are given in eV.*

	6-31G(d,p) in eV	6-311++G(d,p) in eV
Vertical IP-HSE06	8.51	8.70
vertical EA- HSE06	-0.93	-1.30
IP-EA gap	7.58	7.40
optical gap – HSE06	3.51	3.51
HSE06-HOMO	-6.63	-6.92
HSE06-LUMO	-2.64	-2.94
HSE06-gap	3.99	3.98
Vertical IP-B3LYP	8.43	8.69
vertical EA-B3LYP	-0.85	-1.29
IP-EA gap	7.58	7.40
optical gap – B3LYP	3.45	3.45
B3LYP-HOMO	-6.71	-7.07
B3LYP-LUMO	-2.36	-2.73
B3LYP-gap	4.34	4.34
PBE-HOMO	-5.41	-5.78
PBE-LUMO	-3.05	-3.39
PBE-gap	2.36	2.39
PW91-HOMO	-5.46	-5.85
PW91-LUMO	-3.09	-3.45
PW91-gap	2.38	2.41
SVWN-HOMO	-6.02	-6.41
SVWN-LUMO	-3.79	-4.16
SVWN-gap	2.22	2.26

[i] electron affinities are defined such that they are negative when associated with an energy gain upon addition of an electron to be consistent with the sign of the orbital energies.

S3: Discussion of 3N system with an isocyanide docking group attached.

Fig. S4 shows the real-space representations of the highest occupied and lowest unoccupied π-states in the “up” and “down” version of 3N SAMs with an isocyanide docking group attached. As in the equivalent unsubstituted and thiol-substituted systems, strong localization effects are observed as described in the main text. Further, similar to the thiol docking group, isocyanide orbitals hybridize with the frontier π-states.

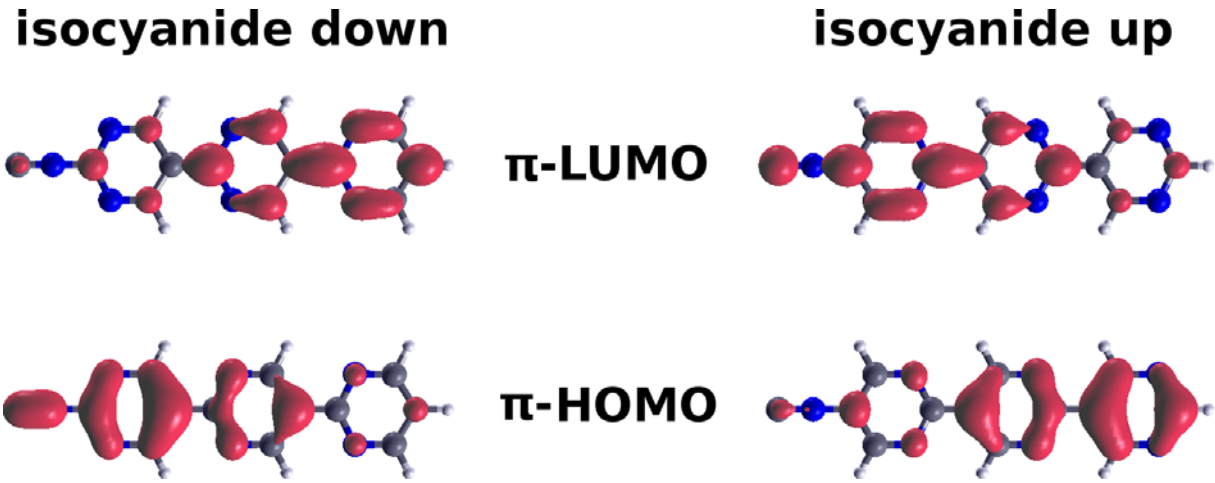

Fig. S4. Real-space representations of highest occupied and lowest unoccupied π-states in the isocyanide-substituted "up" and "down" versions of 3N SAMs.

Further, a gradient in the electrostatic potential across these SAMs is found. As explained in the main text, Fig. S5 shows that its sign depends on the orientation of the pyrimidine rings (positive for "up", black color / negative for "down", gray color). Comparison of this plot with Fig. 3a reveals also an important difference between the isocyanide and the thiol docking group, namely that (unlike the thiol substituent) the isocyanide group shows a sizeable dipole moment itself, directed along the long molecular axis. Consequently, an additional step in the electrostatic potential is introduced for the SAMs of those molecules in the region of the isocyanide. This is reflected in the potentials of Fig. S5 being shifted to much lower energies with respect to the left vacuum energy, E_{vac}^{left} , than for their thiol-substituted counterparts (cf. Fig. 3a of the main text). For instance, the leftmost minimum of the potential on the molecular backbone in Fig. S5 is found at approx. 6.5eV below E_{vac}^{left} . The corresponding minimum in Fig 3a is found only ~4.5eV below E_{vac}^{left} . This additional dipole shift has a profound impact for the alignment of the SAM electronic states with the metallic Fermi energy after adsorption of the SAM.[28]

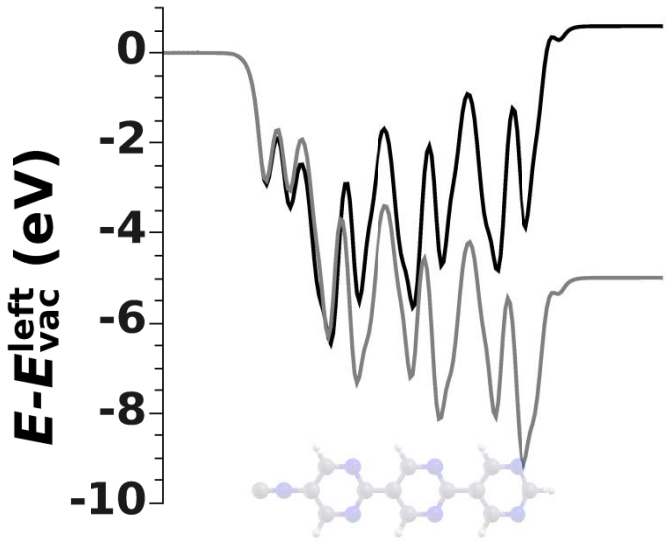

Fig. S5: (x,y)-averaged electrostatic energy E of an electron across the hypothetical free-standing isocyanide-substituted "up" (black) and "down" (gray) version of 3N SAMs at θ=1/2 (cf. Fig. 3a in the main text). The molecule in the background serves as guide to the eye. The zero of the energy axis is set to the left vacuum energy, E_{vac}^{left}.

The main effect discussed in the paper, the reduction of the band gap upon SAM formation, is fully reproduced also when using the isocyanide substituent. Fig. S6 shows the electronic structure of those SAMs. For the "down" variant, the molecular (π-π*) gap of 4.0eV is reduced to 3.3eV, where the HOMO-derived band is of σ-character. The molecular (σ-π*) gap of 3.6eV for the "up" variant transforms to the strongly reduced σ-π* gap of 3.0eV as shown in the right panel of Fig. S6.

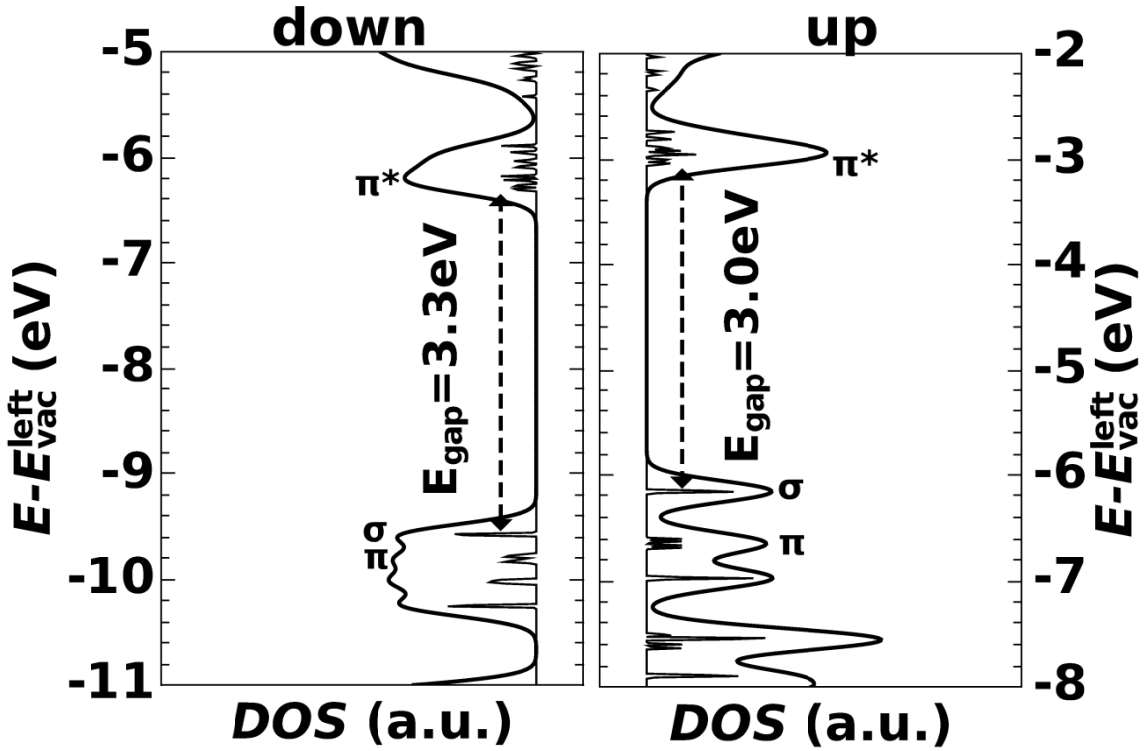

Fig. S6. DOS of the isocyanide-substituted "down" (left) and "up" (right) version of 3N SAMs at θ = ½, aligned at the left vacuum energy, E_{vac}^{left} (cf. Fig. 8a in the main text). The thick black curves are Gaussian-convolutions (σ = 0.1 eV) of the results of the calculation. The character of the frontier stated and the band gap are indicated. The latter is determined from the onsets of the respective non-broadened DOS peaks.

S4: Total energies and geometries of molecules.

All molecules discussed in the main text were obtained by optimizations with the PBE functional using the Gaussian 03[26] package and the aug-cc-pVTZ basis set. The resulting atomic coordinates and total energies are listed below:

3N (terpyrimidine):

Energy: -789.932700453 Hartree
Geometry (in Ångström):

N	-4.890504	1.201949	0.000314
N	-4.890507	-1.201945	0.000272
N	-0.712541	-1.199652	-0.000340
N	-0.712539	1.199647	-0.000327
N	3.461441	1.200446	-0.000013
N	3.461444	-1.200438	0.000042
C	-5.485834	0.000003	0.000339
C	-3.552027	-1.189817	0.000025
C	-2.807052	0.000000	-0.000151
C	-3.552025	1.189818	0.000066
C	-1.330074	-0.000002	-0.000535
C	0.620864	-1.187502	-0.000208
C	1.369778	-0.000003	-0.000193
C	0.620867	1.187496	-0.000195
C	2.846422	-0.000010	-0.000147
C	4.798095	1.184739	0.000219
C	5.534031	0.000000	0.000350
C	4.798115	-1.184732	0.000272
H	6.623069	0.000021	0.000519
H	5.294500	2.159396	0.000274
H	5.294501	-2.159397	0.000372
H	1.130953	-2.153246	-0.000205
H	1.130956	2.153240	-0.000182
H	-3.039556	-2.154019	-0.000140
H	-3.039551	2.154019	-0.000064

$3N^{down}$ (*[2,5':2',5''-terpyrimidine]-2''-thiol*):

Energy: -1187.98405383 Hartree
Geometry (in Ångström):

S	-6.402746	-0.071194	0.000397
N	0.132201	1.198855	-0.000205
N	-4.042255	1.200378	0.000031
N	-4.039142	-1.209729	0.000011
N	0.134500	-1.202244	-0.000397
N	4.308073	-1.198672	0.000088
N	4.306332	1.202445	-0.000144
C	1.465025	1.187096	-0.000158
C	-4.637926	-0.005950	0.000031
C	-2.707001	1.184084	-0.000084
C	-2.705079	-1.194076	-0.000113
C	-1.957059	-0.004135	-0.000199
C	-0.485691	-0.002321	-0.000387
C	1.467258	-1.188028	-0.000337
C	2.215768	0.000236	-0.000284
C	3.691369	0.001436	-0.000350
C	5.644525	-1.181812	0.000487
C	5.642830	1.187417	0.000265
C	6.379917	0.003333	0.000543
H	-2.197744	2.149971	-0.000151
H	1.974597	2.153193	-0.000119
H	6.138652	2.162445	0.000291
H	-2.194962	-2.159447	-0.000193
H	-6.547349	1.277287	0.000590
H	1.978549	-2.153207	-0.000450
H	6.141681	-2.156161	0.000697
H	7.468955	0.004106	0.000815

$3N^{up}$ (*[2,5':2',5''-terpyrimidine]-5-thiol*):

Energy: -1187.97574246 Hartree
Geometry (in Ångström):

S	6.455913	-0.073397	-0.000619
N	2.612083	-1.198941	0.000759

N	2.613901	1.192436	-0.000008
N	-1.566667	1.199017	0.000246
N	-1.568320	-1.199602	0.000075
N	-5.745537	1.204357	0.000040
N	-5.747104	-1.199402	-0.000571
C	4.692677	-0.003758	-0.000036
C	3.943463	-1.192398	0.000560
C	3.943972	1.184101	-0.000163
C	1.988890	-0.003080	0.000362
C	0.515872	-0.001783	0.000336
C	-0.233628	1.186123	0.000386
C	-0.235267	-1.188767	0.000223
C	-2.185775	0.000113	0.000053
C	-3.662556	0.001099	-0.000052
C	-4.407034	1.191272	0.000190
C	-6.341759	0.002859	-0.000362
C	-4.408591	-1.188118	-0.000401
H	4.439400	-2.167763	0.000864
H	4.442066	2.159349	-0.000431
H	6.651352	1.268888	-0.000965
H	0.275732	2.152360	0.000480
H	0.272949	-2.155577	0.000172
H	-3.894018	2.155180	0.000491
H	-3.896839	-2.152697	-0.000584
H	-7.435313	0.003565	-0.000491

3P (terphenyl):

Energy: -693.688219593 Hartree
Geometry (in Ångström):

C	-2.445107	0.352511	2.920773
C	-2.452488	0.000411	1.558822
C	-3.682593	-0.351473	0.974050
C	-4.859593	-0.351966	1.722034
C	-4.835491	0.000838	3.073487
C	-3.621988	0.353430	3.668941
C	-1.203396	0.000175	0.764882
C	-1.193304	0.409766	-0.580181
C	-0.018139	0.412219	-1.325988
C	1.203383	-0.000248	-0.764903
C	1.192773	-0.412488	0.579346
C	0.018647	-0.409622	1.326786
C	2.452480	-0.000456	-1.558835
C	2.711390	1.010457	-2.502212
C	3.888531	1.010863	-3.249974
C	4.835486	-0.000872	-3.073496
C	4.593038	-1.012399	-2.141022
C	3.416295	-1.011584	-1.392636
H	-3.710221	-0.654694	-0.073493
H	-5.799830	-0.638475	1.248799
H	-3.592565	0.640104	4.721099
H	-1.508282	0.655571	3.390421
H	-2.120306	0.749597	-1.044458
H	-0.050488	0.723383	-2.371215
H	2.125346	-0.723806	1.052380
H	0.045428	-0.749290	2.363261
H	3.226445	-1.821523	-0.686938
H	5.320898	-1.812943	-2.001616
H	4.071486	1.811248	-3.968301
H	1.992043	1.820556	-2.630015
H	-5.755825	0.001007	3.658461
H	5.755821	-0.001031	-3.658467

alternative molecule 1 (*2H,2'H,2''H-3,6':3',6''-ter(1',2'-oxazine)*):

Energy: -852.868459063 Hartree
Geometry (in Ångström):

C	0.002697	-0.111078	-0.051486
C	1.169557	-0.426856	-0.663624
C	-0.008574	-0.093776	1.388550
C	1.181678	-0.021358	2.063710
C	1.381413	0.093005	3.474673
C	2.608869	0.097258	4.096371
C	2.657298	0.326599	5.499006
C	1.567168	0.893086	6.124394
C	1.488515	1.361829	7.472795
C	0.358063	1.861710	8.064245
C	0.479699	2.494628	9.346518
C	1.721583	2.875196	9.744259
O	2.364586	0.073548	1.328397
O	0.437678	1.168024	5.382288
O	2.849801	2.519164	9.088355
N	2.260758	-0.803291	0.138258
N	0.252116	0.103716	4.348445
N	2.635894	1.245113	8.330866
H	-0.896096	0.089537	-0.629627
H	-0.950956	-0.148733	1.931217
H	3.163003	-0.637346	-0.308833
H	1.303787	-0.524478	-1.741300
H	3.511387	-0.061831	3.511862
H	3.566031	0.113160	6.059129
H	-0.572592	0.475380	3.869935
H	-0.580696	1.871055	7.515653
H	-0.388468	2.831807	9.907039
H	1.938884	3.592503	10.536345
H	3.493688	1.239495	7.771145

alternative molecule 2 ((1E,NE)-N’-(iminomethyl)-N-(((E-)-(((E)-((methyleneamino)methylene)amino)methylene)amino)methylene) formimidamide):

Energy: -561.393671604 Hartree
Geometry (in Ångström):

C	-0.180090	0.000000	0.088167
C	-2.420847	0.000000	-0.231401
C	-4.673928	0.000000	-0.384985
C	-6.932341	0.000000	-0.357987
C	-9.181744	0.000000	-0.131028
C	-11.407212	0.000000	0.316720
N	-1.139866	0.000000	-0.765255
N	-3.449979	0.000000	-1.012017
N	-5.765990	0.000000	-1.083277
N	-8.080553	0.000000	-0.958545
N	-10.376243	0.000000	-0.620074
N	-12.627838	0.000000	-0.072494
H	-0.340085	0.000000	1.182481
H	0.851053	0.000000	-0.276819
H	-2.517788	0.000000	0.879347
H	-4.695795	0.000000	0.729540
H	-6.860339	0.000000	0.755234
H	-9.006251	0.000000	0.971360
H	-11.105374	0.000000	1.387817
H	-13.248355	0.000000	0.746561

alternative molecule 3 ((1Z,NZ)-N-allylidene-N‘-((Z)-(((Z)-((iminomethyl)imino)methyl)imino)methyl)formimidamide):

Energy: -561.393129219 Hartree
Geometry (in Ångström):

C	-0.058998	0.000000	0.050840
C	-2.327917	0.000000	-0.047675
C	-3.547757	0.000000	-2.015145

C	-5.868432	0.000000	-2.005902
C	-7.095631	0.000000	-3.978506
C	-9.432377	0.000000	-3.973806
N	-1.092160	0.000000	-0.708089
N	-3.481848	0.000000	-0.624292
N	-4.657501	0.000000	-2.687269
N	-7.029279	0.000000	-2.587735
N	-8.202653	0.000000	-4.652137
N	-10.554891	0.000000	-4.592506
H	-0.124357	0.000000	1.154698
H	0.936842	0.000000	-0.402605
H	-2.312642	0.000000	1.057462
H	-2.611268	0.000000	-2.586888
H	-5.857974	0.000000	-0.908622
H	-6.159087	0.000000	-4.550097
H	-9.427381	0.000000	-2.876456
H	-10.363025	0.000000	-5.607869

alternative molecule 4 (*2,5':2',5''-terthiazole)*:

Energy: -1703.91703783 Hartree
Geometry (in Ångström):

S	1.607783	-0.000610	-0.596648
S	-2.802745	0.001010	-0.215800
S	-5.436894	0.002046	-3.778441
C	-0.012746	0.000074	0.044629
C	0.052021	-0.000280	1.427493
C	2.211549	0.000149	1.033587
C	-1.155160	0.000507	-0.832860
C	-2.302301	0.000959	-2.721453
C	-3.384619	0.001231	-1.858943
C	-4.798311	0.001636	-2.133372
C	-6.981891	0.002152	-1.756547
C	-7.035059	0.002285	-3.127322
N	1.301501	-0.000262	1.977367
N	-1.069381	0.000544	-2.152247
N	-5.732232	0.001780	-1.203737
H	-0.818778	-0.000263	2.082435
H	3.283180	0.000223	1.222810
H	-2.386975	0.001019	-3.807904
H	-7.853616	0.002289	-1.104592
H	-7.903519	0.002548	-3.777831

alternative molecule 5 (*2,5':2',5''-terimidazole)*:

Energy: -675.753180454 Hartree
Geometry (in Ångström):

C	-0.071534	0.000026	0.064545
C	0.006236	-0.000269	1.451260
C	2.033830	-0.000023	0.749925
C	-1.139474	0.000189	-0.900394
C	-2.205207	0.000544	-2.775642
C	-3.178071	0.000248	-1.784725
C	-4.617488	0.000121	-1.762606
C	-6.659530	-0.000206	-1.064240
C	-6.733006	0.000113	-2.439343
N	1.316189	-0.000252	1.863362
N	1.242229	0.000147	-0.359913
N	-0.951817	0.000512	-2.224040
N	-2.472802	0.000086	-0.597504
N	-5.349053	-0.000187	-0.648759
N	-5.422661	0.000277	-2.873566
H	-0.809531	-0.000450	2.168595
H	3.118145	0.000040	0.693820
H	-2.344596	0.000761	-3.853051
H	-7.479953	-0.000429	-0.353792
H	-7.567566	0.000211	-3.130451

H	1.512426	0.000348	-1.338937
H	-2.920549	-0.000123	0.314174
H	-5.115729	0.000510	-3.838977

alternative molecule 7 (*2,5':2',5''-teroxazole)*:

Energy: -735.295655205 Hartree
Geometry (in Ångström):

C	-0.029669	0.000021	-0.002480
C	-0.016478	0.000095	1.371023
C	2.001689	-0.000065	0.720422
C	-1.070365	0.000064	-0.988595
C	-2.278696	0.000066	-2.736854
C	-3.129751	0.000241	-1.656829
C	-4.556413	0.000401	-1.510541
C	-6.586834	0.000607	-0.872618
C	-6.596420	0.000647	-2.234304
N	1.293845	-0.000087	1.812941
N	-0.974997	-0.000044	-2.297854
N	-5.278749	0.000520	-0.418209
O	1.277441	-0.000138	-0.433026
O	-2.359095	0.000251	-0.518442
O	-5.293964	0.000428	-2.670657
H	-0.860336	0.000197	2.052282
H	3.081251	-0.000175	0.612992
H	-2.533890	0.000012	-3.791146
H	-7.428966	0.000696	-0.188729
H	-7.361283	0.000742	-3.000562

The unit cells and geometries used in the periodic systems were not fully optimized; for details see main text. The lattice parameters and atomic positions are given in Ängström:

3N (terpyrimidine) SAM:

cell:
a: +5.1135503988 +0.0000000000 +0.0000000000
b: +0.0000000000 +8.8569300817 +0.0000000000
c: +0.0000000000 +0.0000000000 +45.2776661011
atomic positions (in Ångström):

C	+2.5573679244	+4.4288249069	+28.1465040325
C	+2.5576325826	+5.6185903051	+26.2126634312
C	+2.5577666197	+4.4287522705	+25.4677220183
C	+2.5575584408	+3.2389553068	+26.2127286175
C	+2.5581002777	+4.4287125659	+23.9907440066
C	+2.5577233197	+5.6161574894	+22.0397724927
C	+2.5576662548	+4.4286373463	+21.2908920209
C	+2.5576772425	+3.2411594907	+22.0398365471
C	+2.5575699243	+4.4286026571	+19.8142480237
C	+2.5571209024	+3.2437985616	+17.8626084875
C	+2.5569813185	+4.4285167852	+17.1266390436
C	+2.5571009018	+5.6132695606	+17.8625215913
H	+2.5567751990	+4.4284650410	+16.0376010510
H	+2.5570354085	+2.2691275479	+17.3662310076
H	+2.5569975571	+6.5879205471	+17.3661080772
H	+2.5577163837	+6.5818870877	+21.5296562271
H	+2.5576334063	+2.2754010901	+21.5297748142
H	+2.5577935439	+6.5827778338	+25.7001652034
H	+2.5576575448	+2.2747398369	+25.7002818361
H	+2.5570001978	+4.4288547868	+29.2400650453
N	+2.5573558932	+3.2268620993	+27.5512079671

N +2.5574313728 +5.6307560976 +27.5511430958
N +2.5579009372 +5.6283451333 +23.3731771438
N +2.5578545217 +3.2290461347 +23.3732428844
N +2.5573982428 +3.2281292958 +19.1992629217
N +2.5573766803 +5.6290132953 +19.1991921387

$3N^{down}$ (*[2,5':2',5''-terpyrimidine]-2''-thiol*) SAM:

cell:
a: +5.1135503988 +0.0000000000 +0.0000000000
b: +0.0000000000 +8.8569300817 +0.0000000000
c: +0.0000000000 +0.0000000000 +45.2776661011
atomic positions (in Ångström):
S +2.5564091990 +4.3632210410 +16.2351800000
C +2.5569641990 +5.6215110410 +24.1029510000
C +2.5567751990 +4.4284650410 +18.0000000000
C +2.5568901990 +5.6184990410 +19.9309250000
C +2.5569191990 +3.2403390410 +19.9328470000
C +2.5570051990 +4.4302800410 +20.6808670000
C +2.5571931990 +4.4320940410 +22.1522350000
C +2.5571431990 +3.2463870410 +24.1051840000
C +2.5570901990 +4.4346510410 +24.8536940000
C +2.5571561990 +4.4358510410 +26.3292950000
C +2.5563191990 +3.2526030410 +28.2824510000
C +2.5565411990 +5.6218320410 +28.2807560000
C +2.5562631990 +4.4377480410 +29.0178430000
H +2.5569571990 +6.5843860410 +20.4401820000
H +2.5569251990 +6.5876080410 +24.6125230000
H +2.5565151990 +6.5968600410 +28.7765780000
H +2.5569991990 +2.2749680410 +20.4429640000
H +2.5562161990 +5.7117020410 +16.0905770000
H +2.5572561990 +2.2812080410 +24.6164750000
H +2.5561091990 +2.2782540410 +28.7796070000
H +2.5559911990 +4.4385210410 +30.1068810000
N +2.5570111990 +5.6332700410 +22.7701270000
N +2.5567751990 +5.6347930410 +18.5956710000
N +2.5567951990 +3.2246860410 +18.5987840000
N +2.5572031990 +3.2321710410 +22.7724260000
N +2.5567181990 +3.2357430410 +26.9459990000
N +2.5569501990 +5.6368600410 +26.9442580000

$3N^{up}$ (*[2,5':2',5''-terpyrimidine]-5-thiol*) SAM:

cell:
a: +5.1135503988 +0.0000000000 +0.0000000000
b: +0.0000000000 +8.8569300817 +0.0000000000
c: +0.0000000000 +0.0000000000 +45.2776661011
atomic positions (in Ångström):
S +2.5561921990 +4.3588260410 +16.2367640000
C +2.5567751990 +4.4284650410 +18.0000000000
C +2.5573711990 +3.2398250410 +18.7492140000
C +2.5566481990 +5.6163240410 +18.7487050000
C +2.5571731990 +4.4291430410 +20.7037870000
C +2.5571471990 +4.4304400410 +22.1768050000
C +2.5571971990 +5.6183460410 +22.9263050000
C +2.5570341990 +3.2434560410 +22.9279440000
C +2.5568641990 +4.4323360410 +24.8784520000
C +2.5567591990 +4.4333220410 +26.3552330000
C +2.5570011990 +5.6234950410 +27.0997110000
C +2.5564491990 +4.4350820410 +29.0344360000
C +2.5564101990 +3.2441050410 +27.1012680000
H +2.5576751990 +2.2644600410 +18.2532770000
H +2.5563801990 +6.5915720410 +18.2506110000
H +2.5558461990 +5.7011110410 +16.0413250000
H +2.5572911990 +6.5845830410 +22.4169450000
H +2.5569831990 +2.2766460410 +22.4197280000
H +2.5573021990 +6.5874030410 +26.5866950000
H +2.5562271990 +2.2795260410 +26.5895160000

H +2.5563201990 +4.4357880410 +30.1279900000
N +2.5575701990 +3.2332820410 +20.0805940000
N +2.5568031990 +5.6246590410 +20.0787760000
N +2.5570571990 +5.6312400410 +24.2593440000
N +2.5568861990 +3.2326210410 +24.2609970000
N +2.5568511990 +5.6365800410 +28.4382140000
N +2.5562401990 +3.2328210410 +28.4397810000

3P (terphenyl) SAM:

cell:
a: +5.1135503988 +0.0000000000 +0.0000000000
b: +0.0000000000 +8.8569300817 +0.0000000000
c: +0.0000000000 +0.0000000000 +45.2776661011
atomic positions (in Ångström):
C +3.2851715584 +3.4669075962 +26.4865536430
C +2.5579795758 +4.4289072704 +25.7622002329
C +1.8309909123 +5.3909798787 +26.4866605368
C +1.8304900654 +5.3909138924 +27.8812246451
C +2.5583808671 +4.4290531992 +28.5858350110
C +3.2860719669 +3.4671213267 +27.8811160233
C +2.5577571283 +4.4288284097 +24.2821422786
C +2.5539421060 +5.6305302301 +23.5521016700
C +2.5565767207 +5.6304691712 +22.1602540021
C +2.5573573579 +4.4286899611 +21.4303310469
C +2.5583531431 +3.2269833715 +22.1603721722
C +2.5613787265 +3.2270557154 +23.5522189569
C +2.5571644469 +4.4286118688 +19.9502731643
C +3.2804591935 +5.3933928261 +19.2257167069
C +3.2809687674 +5.3931819408 +17.8311526879
C +2.5567751990 +4.4284650410 +17.1266380000
C +1.8327763370 +3.4638213300 +17.8314527443
C +1.8336677949 +3.4637570252 +19.2260156000
H +1.2371953553 +6.1308167484 +25.9480504174
H +1.2507172332 +6.1410589001 +28.4208822393
H +3.8659995175 +2.7170336571 +28.4206868492
H +3.8788162160 +2.7270145923 +25.9478514513
H +2.5673643278 +6.5822597835 +24.0853948825
H +2.5395110409 +6.5820887383 +21.6268705224
H +2.5752741076 +2.2753111398 +21.6270747814
H +2.5481116755 +2.2753764474 +24.0856067652
H +1.2428643976 +2.7216486416 +19.7647923312
H +1.2557323846 +2.7114588793 +17.2919567498
H +3.8578644003 +6.1454870278 +17.2914204913
H +3.8714125512 +6.1355570001 +19.7642522869
H +2.5585393356 +4.4291119288 +29.6763437236
H +2.5566271758 +4.4284068684 +16.0361300527

3N^{down} SAM on Au(111):

cell:
a: +5.1135503988 +0.0000000000 +0.0000000000
b: +0.0000000000 +8.8569300817 +0.0000000000
c: +0.0000000000 +0.0000000000 +45.2776661011
atomic positions (in Ångström):
Au +1.7044997544 +0.0000000000 +4.8211658864
Au +1.7044997544 +2.9522805041 +4.8211658864
Au +1.7045000000 +5.9046500000 +4.8211658864
Au +4.2612749538 +1.4761845367 +4.8211658864
Au +4.2612749538 +4.4284650408 +4.8211658864
Au +4.2612749538 +7.3807455450 +4.8211658864
Au +0.0000000000 +0.0000000000 +2.4105829432
Au +0.0000000000 +2.9522805041 +2.4105829432
Au +0.0000000000 +5.9046495776 +2.4105829432
Au +2.5567751994 +1.4761845367 +2.4105829432
Au +2.5567751994 +4.4284650408 +2.4105829432
Au +2.5567751994 +7.3807455450 +2.4105829432
Au +3.4090506444 +0.0000000000 +0.0000000000

Au +3.4090506444 +2.9522805041 +0.0000000000
Au +3.4090506444 +5.9046495776 +0.0000000000
Au +0.8522754450 +1.4761845367 +0.0000000000
Au +0.8522754450 +4.4284650408 +0.0000000000
Au +0.8522754450 +7.3807455450 +0.0000000000
Au +3.4090506444 +0.0000000000 +7.2317490000
Au +0.8522754450 +1.4761845367 +7.2317490000
Au +3.4090506444 +2.9522805041 +7.2317490000
Au +0.8522754450 +4.4284650408 +7.2317490000
Au +3.4090506444 +5.9046495776 +7.2317490000
Au +0.8522754450 +7.3807455450 +7.2317490000
Au +2.5567751994 +7.3807455450 +9.6423319432
Au +0.0000000000 +5.9046495776 +9.6423319432
Au +2.5567751994 +4.4284650408 +9.6423319432
Au +0.0000000000 +2.9522805041 +9.6423319432
Au +2.5567751994 +1.4761845367 +9.6423319432
Au +0.0000000000 +0.0000000000 +9.6423319432
S +1.6614240000 +5.8847320000 +11.2977660000
C +1.6619790000 +7.1430220000 +19.1655370000
C +1.6617900000 +5.9499760000 +13.0625860000
C +1.6619050000 +7.1400100000 +14.9935110000
C +1.6619340000 +4.7618500000 +14.9954330000
C +1.6620200000 +5.9517910000 +15.7434530000
C +1.6622080000 +5.9536050000 +17.2148210000
C +1.6621580000 +4.7678980000 +19.1677700000
C +1.6621050000 +5.9561620000 +19.9162800000
C +1.6621710000 +5.9573620000 +21.3918810000
C +1.6613340000 +4.7741140000 +23.3450370000
C +1.6615560000 +7.1433430000 +23.3433420000
C +1.6612780000 +5.9592590000 +24.0804290000
N +1.6619720000 +8.1058970000 +15.5027680000
N +1.6619400000 +8.1091190000 +19.6751090000
N +1.6615300000 +8.1183710000 +23.8391640000
N +1.6620140000 +3.7964790000 +15.5055500000
N +1.6622710000 +3.8027190000 +19.6790610000
N +1.6611240000 +3.7997650000 +23.8421930000
N +1.6610060000 +5.9600320000 +25.1694670000
H +1.6620260000 +7.1547810000 +17.8327130000
H +1.6617900000 +7.1563040000 +13.6582570000
H +1.6618100000 +4.7461970000 +13.6613700000
H +1.6622180000 +4.7536820000 +17.8350120000
H +1.6617330000 +4.7572540000 +22.0085850000
H +1.6619650000 +7.1583710000 +22.0068440000

3N^{up} SAM on Au(111):

cell:
a: +5.1135503988 +0.0000000000 +0.0000000000
b: +0.0000000000 +8.8569300817 +0.0000000000
c: +0.0000000000 +0.0000000000 +45.2776661011
atomic positions (in Ångström):
Au +1.7044997544 +0.0000000000 +4.8211658864
Au +1.7044997544 +2.9522805041 +4.8211658864
Au +1.7045000000 +5.9046500000 +4.8211658864
Au +4.2612749538 +1.4761845367 +4.8211658864
Au +4.2612749538 +4.4284650408 +4.8211658864
Au +4.2612749538 +7.3807455450 +4.8211658864
Au +0.0000000000 +0.0000000000 +2.4105829432
Au +0.0000000000 +2.9522805041 +2.4105829432
Au +0.0000000000 +5.9046495776 +2.4105829432
Au +2.5567751994 +1.4761845367 +2.4105829432
Au +2.5567751994 +4.4284650408 +2.4105829432
Au +2.5567751994 +7.3807455450 +2.4105829432
Au +3.4090506444 +0.0000000000 +0.0000000000
Au +3.4090506444 +2.9522805041 +0.0000000000
Au +3.4090506444 +5.9046495776 +0.0000000000
Au +0.8522754450 +1.4761845367 +0.0000000000
Au +0.8522754450 +4.4284650408 +0.0000000000

Au	+0.8522754450	+7.3807455450	+0.0000000000
Au	+3.4090506444	+0.0000000000	+7.2317490000
Au	+0.8522754450	+1.4761845367	+7.2317490000
Au	+3.4090506444	+2.9522805041	+7.2317490000
Au	+0.8522754450	+4.4284650408	+7.2317490000
Au	+3.4090506444	+5.9046495776	+7.2317490000
Au	+0.8522754450	+7.3807455450	+7.2317490000
Au	+2.5567751994	+7.3807455450	+9.6423319432
Au	+0.0000000000	+5.9046495776	+9.6423319432
Au	+2.5567751994	+4.4284650408	+9.6423319432
Au	+0.0000000000	+2.9522805041	+9.6423319432
Au	+2.5567751994	+1.4761845367	+9.6423319432
Au	+0.0000000000	+0.0000000000	+9.6423319432
S	+1.6614240000	+5.8847320000	+11.2977660000
C	+1.6620070000	+5.9543710000	+13.0610020000
C	+1.6626030000	+4.7657310000	+13.8102160000
C	+1.6618800000	+7.1422300000	+13.8097070000
C	+1.6624050000	+5.9550490000	+15.7647890000
C	+1.6623790000	+5.9563460000	+17.2378070000
C	+1.6624290000	+7.1442520000	+17.9873070000
C	+1.6622660000	+4.7693620000	+17.9889460000
C	+1.6620960000	+5.9582420000	+19.9394540000
C	+1.6619910000	+5.9592280000	+21.4162350000
C	+1.6622330000	+7.1494010000	+22.1607130000
C	+1.6616810000	+5.9609880000	+24.0954380000
C	+1.6616420000	+4.7700110000	+22.1622700000
H	+1.6629070000	+3.7903660000	+13.3142790000
H	+1.6616120000	+8.1174780000	+13.3116130000
H	+1.6625230000	+8.1104890000	+17.4779470000
H	+1.6622150000	+3.8025520000	+17.4807300000
H	+1.6625340000	+8.1133090000	+21.6476970000
H	+1.6614590000	+3.8054320000	+21.6505180000
H	+1.6615520000	+5.9616940000	+25.1889920000
N	+1.6628020000	+4.7591880000	+15.1415960000
N	+1.6620350000	+7.1505650000	+15.1397780000
N	+1.6622890000	+7.1571460000	+19.3203460000
N	+1.6621180000	+4.7585270000	+19.3219990000
N	+1.6620830000	+7.1624860000	+23.4992160000
N	+1.6614720000	+4.7587270000	+23.5007830000

S5: Complete citations of reference 11, 123 and 132 in the main text.

Ref 11:

Smits, E. C. P.; Mathijssen, S. G. J.; van Hal, P. A.; Setayesh, S.; Geuns, T. C. T.; Mutsaers, K. A. H. A.; Cantatore, E.; Wondergem, H. J.; Werzer, O.; Resel, R.; Kemerink, M.; Kirchmeyer, S.; Muzafarov, A. M.; Ponomarenko, S. A.; de Boer, B.; Blom, P. W. M.; de Leeuw, D. M. *Nature* **2008**, *455*, 956-959.

Ref 123:

Frisch, M. J.; Trucks, G. W.; Schlegel, H. B.; Scuseria, G. E.; Robb, M. A.; Cheeseman, J. R.; Montgomery, J.; Vreven, T.; Kudin, K. N.; Burant, J. C.; Millam, J. M.; Iyengar, S. S.; Tomasi, J.; Barone, V.; Mennucci, B.; Cossi, M.; Scalmani, G.; Rega, N.; Petersson, G. A.;

Nakatsuji, H.; Hada, M.; Ehara, M.; Toyota, K.; Fukuda, R.; Hasegawa, J.; Ishida, M.; Nakajima, T.; Honda, Y.; Kitao, O.; Nakai, H.; Klene, M.; Li, X.; Knox, J. E.; Hratchian, H. P.; Cross, J. B.; Bakken, V.; Adamo, C.; Jaramillo, J.; Gomperts, R.; Stratmann, R. E.; Yazyev, O.; Austin, A. J.; Cammi, R.; Pomelli, C.; Ochterski, J. W.; Ayala, P. Y.; Morokuma, K.; Voth, G. A.; Salvador, P.; Dannenberg, J. J.; Zakrzewski, V. G.; Dapprich, S.; Daniels, A. D.; Strain, M. C.; Farkas, O.; Malick, D. K.; Rabuck, A. D.; Raghavachari, K.; Foresman, J. B.; Ortiz, J. V.; Cui, Q.; Baboul, A. G.; Clifford, S.; Cioslowski, J.; Stefanov, B. B.; Liu, G.; Liashenko, A.; Piskorz, P.; Komaromi, I.; Martin, R. L.; Fox, D. J.; Keith, T.; Al-Laham, M. A.; Peng, C. Y.; Nanayakkara, A.; Challacombe, M.; Gill, P. M. W.; Johnson, B.; Chen, W.; Wong, M. W.; Gonzalez, C.; Pople, J. A. *Gaussian 03, Revision C.02*; Gaussian Inc.: Wallingford CT, 2004.

Ref. 132:

Frisch, M. J.; Trucks, G. W.; Schlegel, H. B.; Scuseria, G. E.; Robb, M. A.; Cheeseman, J. R.; Scalmani, G.; Barone, V.; Mennucci, B.; Petersson, G. A.; Nakatsuji, H.; Caricato, M.; Li, X.; Hratchian, H. P.; Izmaylov, A. F.; Bloino, J.; Zheng, G.; Sonnenberg, J. L.; Hada, M.; Ehara, M.; Toyota, K.; Fukuda, R.; Hasegawa, J.; Ishida, M.; Nakajima, T.; Honda, Y.; Kitao, O.; Nakai, H.; Vreven, T.; Montgomery, J.; Peralta, J. E.; Ogliaro, F.; Bearpark, M.; Heyd, J. J.; Brothers, E.; Kudin, K. N.; Staroverov, V. N.; Kobayashi, R.; Normand, J.; Raghavachari, K.; Rendell, A.; Burant, J. C.; Iyengar, S. S.; Tomasi, J.; Cossi, M.; Rega, N.; Millam, J. M.; Klene, M.; Knox, J. E.; Cross, J. B.; Bakken, V.; Adamo, C.; Jaramillo, J.; Gomperts, R.; Stratmann, R. E.; Yazyev, O.; Austin, A. J.; Cammi, R.; Pomelli, C.; Ochterski, J. W.; Martin, R. L.; Morokuma, K.; Zakrzewski, V. G.; Voth, G. A.; Salvador, P.; Dannenberg, J. J.; Dapprich, S.; Daniels, A. D.; Farkas, Ö.; Foresman, J. B.; Ortiz, J. V.; Cioslowski, J.; Fox, D. J. *Gaussian 09, Revision A.02*; Gaussian Inc.: Wallingford CT, 2009.

Acknowledgements:

The authors are grateful to Z.Y. Ma from the Institute of Chemistry of the Chinese Academy of Sciences for support with the Gaussian HSE06 calculations.

References:

(1) Perdew, J. P.; Zunger, A. *Phys. Rev. B* **1981**, *23*, 5048-5079.

(2) Körzdörfer, T.; Kümmel, S.; Marom, N.; Kronik, L. *Phys. Rev. B* **2009**, *79*, 201205.

(3) Körzdörfer, T.; Kümmel, S.; Marom, N.; Kronik, L. *Phys. Rev. B* **2010**, *82*, 129903.

(4) Körzdörfer, T. *J. Chem. Phys.* **2011**, *134*, 094111.

(5) Kümmel, S.; Kronik, L. *Rev. Mod. Phys.* **2008**, *80*, 3-60.

(6) Körzdörfer, T.; Kümmel, S. *Phys. Rev. B* **2010**, *82*, 155206.

(7) Dori, N.; Menon, M.; Kilian, L.; Sokolowski, M.; Kronik, L.; Umbach, E. *Phys. Rev. B* **2006**, *73*, 195208.

(8) Palummo, M.; Hogan, C.; Sottile, F.; Bagalá, P.; Rubio, A. *J. Chem. Phys.* **2009**, *131*, 084102.

(9) Stenuit, G.; Castellarin-Cudia, C.; Plekan, O.; Feyer, V.; Prince, K. C.; Goldoni, A.; Umari, P. *Phys. Chem. Chem. Phys.* **2010**, *12*, 10812-10817.

(10) Blase, X.; Attaccalite, C.; Olevano, V. *Phys. Rev. B* **2011**, *83*, 115103.

(11) Marom, N.; Hod, O.; Scuseria, G. E.; Kronik, L. *J. Chem. Phys.* **2008**, *128*, 164107.

(12) Marom, N.; Kronik, L. *Appl. Phys. A* **2008**, *95*, 159-163.

(13) Arantes, J. T.; Lima, M. P.; Fazzio, A.; Xiang, H.; Wei, S.-H.; Dalpian, G. M. *J. Phys. Chem. B* **2009**, *113*, 5376-5380.

(14) Sauther, J.; Wüsten, J.; Lach, S.; Ziegler, C. *J. Chem. Phys.* **2009**, *131*, 034711.

(15) Stradi, D.; Díaz, C.; Martín, F.; Alcamí, M. *Theor Chem Acc* **2010**, *128*, 497-503.

(16) Sánchez-Friera, P.; Godby, R. *Phys. Rev. Lett.* **2000**, *85*, 5611-5614.

(17) Slater, J. C. *The Self-consistent Field for Molecules and Solids. Quantum Theory of Molecules and Solids Volume 4.*; McGraw-Hill: New York, 1974.

(18) Vosko, S. H.; Wilk, L.; Nusair, M. *Can. J. Phys.* **1980**, *58*, 1200-1211.

(19) Perdew, J. P.; Burke, K.; Ernzerhof, M. *Phys. Rev. Lett.* **1996**, *77*, 3865-3868.

(20) Perdew, J. P.; Burke, K.; Ernzerhof, M. *Phys. Rev. Lett.* **1997**, *78*, 1396-1396.

(21) Perdew, J. P.; Wang, Y. *Phys. Rev. B* **1992**, *45*, 13244-13249.

(22) Becke, A. D. *J. Chem. Phys.* **1993**, *98*, 5648.

(23) Heyd, J.; Scuseria, G. E.; Ernzerhof, M. *J. Chem. Phys.* **2003**, *118*, 8207-8215.

(24) Heyd, J.; Scuseria, G. E. *J. Chem. Phys.* **2004**, *121*, 1187-1192.

(25) Heyd, J.; Scuseria, G. E.; Ernzerhof, M. *J. Chem. Phys.* **2006**, *124*, 219906.

(26) Frisch, M. J.; Trucks, G. W.; Schlegel, H. B.; Scuseria, G. E.; Robb, M. A.; Cheeseman, J. R.; Montgomery, J.; Vreven, T.; Kudin, K. N.; Burant, J. C.; Millam, J. M.; Iyengar, S. S.; Tomasi, J.; Barone, V.; Mennucci, B.; Cossi, M.; Scalmani, G.; Rega, N.; Petersson, G. A.; Nakatsuji, H.; Hada, M.; Ehara, M.; Toyota, K.; Fukuda, R.; Hasegawa, J.; Ishida, M.; Nakajima, T.; Honda, Y.; Kitao, O.; Nakai, H.; Klene, M.; Li, X.; Knox, J. E.; Hratchian, H. P.; Cross, J. B.; Bakken, V.; Adamo, C.; Jaramillo, J.; Gomperts, R.; Stratmann, R. E.; Yazyev, O.; Austin, A. J.; Cammi, R.; Pomelli, C.; Ochterski, J. W.; Ayala, P. Y.; Morokuma, K.; Voth, G. A.; Salvador, P.; Dannenberg, J. J.; Zakrzewski, V. G.; Dapprich, S.; Daniels, A. D.; Strain, M. C.; Farkas, O.; Malick, D. K.; Rabuck, A. D.; Raghavachari, K.; Foresman, J. B.; Ortiz, J. V.; Cui, Q.; Baboul, A. G.; Clifford, S.; Cioslowski, J.; Stefanov, B. B.; Liu, G.; Liashenko, A.; Piskorz, P.; Komaromi, I.; Martin, R. L.; Fox, D. J.; Keith, T.; Al-Laham, M. A.; Peng, C. Y.; Nanayakkara, A.; Challacombe, M.; Gill, P. M. W.; Johnson, B.; Chen, W.; Wong, M. W.; Gonzalez, C.; Pople, J. A. *Gaussian 03, Revision C.02*; Gaussian Inc.: Wallingford CT, 2004.

(27) Frisch, M. J.; Trucks, G. W.; Schlegel, H. B.; Scuseria, G. E.; Robb, M. A.;

Cheeseman, J. R.; Scalmani, G.; Barone, V.; Mennucci, B.; Petersson, G. A.; Nakatsuji, H.; Caricato, M.; Li, X.; Hratchian, H. P.; Izmaylov, A. F.; Bloino, J.; Zheng, G.; Sonnenberg, J. L.; Hada, M.; Ehara, M.; Toyota, K.; Fukuda, R.; Hasegawa, J.; Ishida, M.; Nakajima, T.; Honda, Y.; Kitao, O.; Nakai, H.; Vreven, T.; Montgomery, J.; Peralta, J. E.; Ogliaro, F.; Bearpark, M.; Heyd, J. J.; Brothers, E.; Kudin, K. N.; Staroverov, V. N.; Kobayashi, R.; Normand, J.; Raghavachari, K.; Rendell, A.; Burant, J. C.; Iyengar, S. S.; Tomasi, J.; Cossi, M.; Rega, N.; Millam, J. M.; Klene, M.; Knox, J. E.; Cross, J. B.; Bakken, V.; Adamo, C.; Jaramillo, J.; Gomperts, R.; Stratmann, R. E.; Yazyev, O.; Austin, A. J.; Cammi, R.; Pomelli, C.; Ochterski, J. W.; Martin, R. L.; Morokuma, K.; Zakrzewski, V. G.; Voth, G. A.; Salvador, P.; Dannenberg, J. J.; Dapprich, S.; Daniels, A. D.; Farkas, Ö.; Foresman, J. B.; Ortiz, J. V.; Cioslowski, J.; Fox, D. J. *Gaussian 09, Revision A.02*; Gaussian Inc.: Wallingford CT, 2009.

(28) Heimel, G.; Romaner, L.; Zojer, E.; Brédas, J.-L. *Nano Lett.* **2007**, *7*, 932-940.